Journal of Engineering Research and Reports

Volume 26, Issue 5, Page 262-272, 2024; Article no.JERR.116068
ISSN: 2582-2926

Structural Optimization of 60T Electric Mining Vehicle Frame: Finite Element Simulation Model and Analysis

Fan Jialin [a*]

[a] *School of Mechanical Engineering, North China University of Water Resources and Electric Power, Zhengzhou, China.*

Author's contribution

The sole author designed, analyzed, interpreted and prepared the manuscript.

Article Information

DOI: 10.9734/JERR/2024/v26i51152

Open Peer Review History:
This journal follows the Advanced Open Peer Review policy. Identity of the Reviewers, Editor(s) and additional Reviewers, peer review comments, different versions of the manuscript, comments of the editors, etc are available here: https://www.sdiarticle5.com/review-history/116068

Original Research Article

Received: 18/02/2024
Accepted: 22/04/2024
Published: 24/04/2024

ABSTRACT

Based on the research under the ore loading condition of the electric mine vehicle, this paper measures the physical frame of the 60T electric mine vehicle by means of rangefinder, ruler and drawings, and uses the software CATIA to complete the three-dimensional model of the frame and carriage of the electric mine vehicle, combined with the characteristics of ANSYS workbench software. The structure of the model is simplified. By comprehensively applying relevant knowledge of automobile dynamics, the frame load under full load condition is calculated, and the electric mine vehicle frame is applied by using ANSYS workbench software to simulate and optimize the three conditions of stationary, high-speed driving and turning before the mine car, and the position where the stress concentration and deformation of the frame structure are greatest. By increasing the thickness of the support plate and increasing its stress area, the overall weight was increased by 90.35kg, accounting for 0.9% of the total weight, and the weight increase was very small. Mechanical analysis was carried out on the three working conditions of the optimized frame of the mine car, and the stress was reduced by 25%, 24.1% and 39.2% respectively, effectively eliminating the stress concentration. The actual use of the vehicle can extend the service life of the frame, while improving the economy and stability of the vehicle.

**Corresponding author: Email: 1003719365@qq.com;*

Keywords: Electric mine vehicles; frame modeling; finite element simulation; optimal design.

1. INTRODUCTION

Since the power of pure electric mine vehicles comes from the energy storage of batteries, and the energy density of batteries is insufficient, higher requirements are put forward for the design optimization of electric mine vehicles, hoping to reduce the vehicle assembly mass as much as possible and reduce the energy consumption of ore transport per unit mass [1].

As the main load-bearing parts of mining vehicles, the frame and carriage need to withstand various forces and moments, and their structural strength and stiffness directly affect the service life of mining vehicles. The carriage and carriage of pure electric mining vehicles are the main load-bearing parts [2,3]. Therefore, it is of great significance to analyze and check the limit conditions of the carriage frame under different operating conditions in order to improve its safety and economy [5,6].

2. 3D MODELING OF FRAME BODY

When establishing the frame model in the early stage, we should not only consider its accuracy, but also consider the problem that the loading time is too long when analyzing with ANSYS software. Therefore, in the process of modeling, on the one hand, it is necessary to truly reflect the frame structure to ensure the accuracy and authenticity of the finite element software analysis results.

In the process of analysis, some connection components that do not affect the result will greatly increase the analysis time, so they should be simplified or omitted in the early modeling process to improve the actual work efficiency. In this design, CATIA and ANSYS software will be combined to finally complete the 3D model and finite element model modeling and entity conversion of the frame structure [6]. On the one hand, without affecting the analysis results, some assembly parts, fixed parts and other parts will be ignored to reduce the time of finite element analysis.

The frame, carriage and front and rear axle models drawn [7] were assembled so that ANSYS could simulate the actual working conditions. The assembly relationship was that the carriage was fixed on the frame, which was mainly restricted by the position deviation constraints in three directions. The frame carriage was assembled, as shown in Fig. 1.

3. LOAD CALCULATION UNDER DIFFERENT WORKING CONDITIONS

The electric mine car in this design is used for mining and transporting ore and other goods all the year round, and the driving road condition is very complicated. During the preliminary analysis of the load, it is found that the overall weight of the frame due to the gravity can be simulated by adding downward acceleration ($9.8m/s^2$) in the vertical direction.

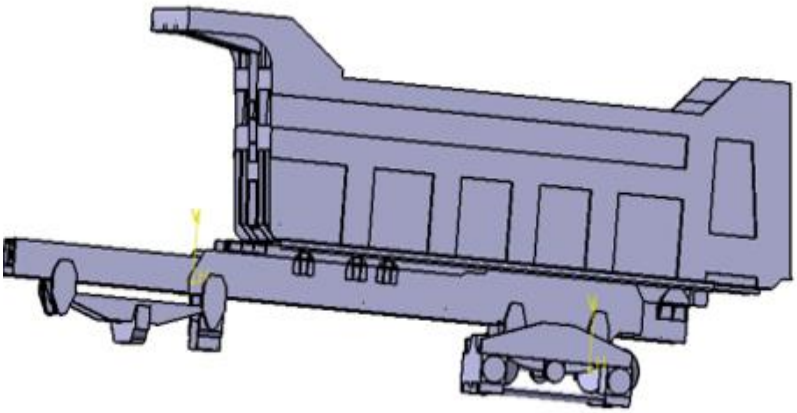

Fig. 1. Body structure of the frame

After consulting relevant literature [8], it is found that the typical road conditions of the electric mine car are static condition, high-speed driving condition and turning condition. The static condition reflects the size and distribution of the overall load of the mine car. The high-speed driving condition and turning condition are its limit states in the face of different grades of road surface and different driving operations. Can more accurately reflect whether its structure is safe.

3.1 Static Load Analysis and Calculation

According to the model drawn in Chapter 2, the weight of the carriage is 9.34T, and its gravity is $m_1g=9.34\times10^4$N; the weight of the cab is 0.6t according to the data provided by the enterprise, and its gravity is 6000N, the total body mass is 9.94T, and the gravity is $m_3g=m_1g+m_2g=9.94\times10^4$N.

the mass of the cab acts on the two longitudinal beams of the lower frame, and is added to the upper surface of the longitudinal beam in the way of uniform load. under full load, the load of the mine vehicle is 60t, and the mass of the carriage and the load of the goods are 69.34t in total, which acts on the bottom floor of the carriage. the mine car is overloaded in the actual loading, so a certain load margin is selected in the calculation. some bolt holes, threaded holes, unnecessary chamfer and other structures on the frame are simplified in the modeling, which is convenient for finite element analysis and calculation.

in this design, the impact load acting on the bottom of the carriage is applied to 70t, that is, the force size is 7×105n. under static conditions, the car can only bear the weight of the goods and its own weight, the bottom load of the car is 70t, the impact load of the cab is 0.6t, the force is 6000n, and the total bearing capacity of the frame is 7.06×105n.

3.2 High-Speed Driving Load Calculation

The mining car is subject to different loads when driving on different grades of road surface, and the road level is divided into eight grades A, B, C, D, E, F, G, H according to its risk and driving difficulty, etc. This design of electric mining car is mostly driven on D grade road, that is, there are more pits and stones about 10cm, long-distance mud road with 10cm depth, and unpaved road with slope below 18 degrees.

When driving at high speed in class D road conditions, the speed of mining car is generally not more than 40km/h [9], and the worst road conditions are taken, and the dynamic load coefficient is 1.5, as shown in Fig. 2.

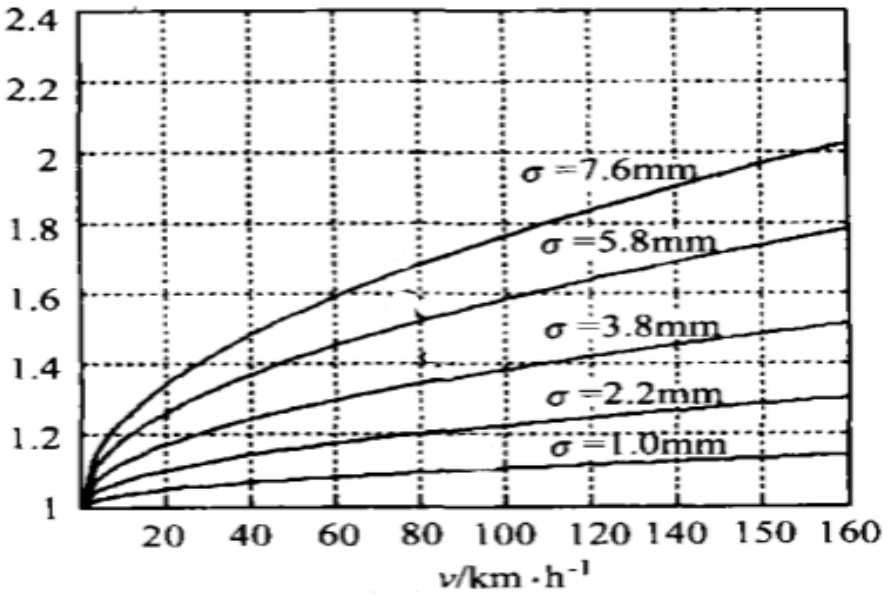

Fig. 2. Selection diagram of dynamic load coefficient

3.3 Calculation of Turning Load

When turning a large mining car, in addition to the maximum force when going straight, it is also subjected to a lateral acceleration. In view of such a large tonnage mining car, its steering acceleration is $2m/s^2$, and it is also in a driving state, so a maximum dynamic load coefficient of 1.5 is also given to the worst ground (Fig. 2). The added load is calculated as follows:

The acceleration orientation left is $2m/s^2$, the force on the bottom of the carriage is $F_1=1.05\times10^6N$ in the vertical direction, and the lateral force is: $F_2=m_4\times a=1.05\times10^5\times2=2.1\times10^5N$. The vertical force on the lower frame is $F_3=9000N$, the lateral force is $F_4=900\times2=1800N$, and the vertical force on the frame is $F_5=F_1+F_3=1.059\times10^6N$. The lateral force is $F_6=F_2+F_4=211800N$.

3.4 Selection of Safety Factor

Compared with traditional vehicles, mining vehicles have harsh driving conditions, large load bearing capacity and long working time. When safety factor is selected for stress check on the frame, due to the harsh working environment of mining vehicles, the safety factor is set as 3, and the stress value of the frame structure conforms to the normal distribution curve and meets the principle of 3□, that is, the safe range of the frame stress is less than □s/3, The yield limit of the Q235 material used in the frame is □s=235MPa, so the safe stress value should not be greater than □s/3, that is 78.33MPa, its probability density curve is shown in Fig. 3.

4. FINITE ELEMENT ANALYSIS UNDER DIFFERENT WORKING CONDITIONS

4.1 Model Pre-Processing

After the simplified model materials are defined, grid division is carried out. Hexahedron division method and minimum size method are used to divide the model into blocks and grids. The grid division model is shown in Fig. 4.

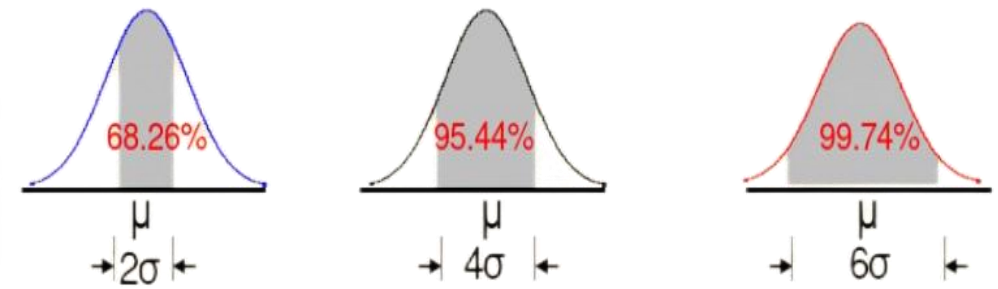

Fig. 3. Normal distribution probability density curve

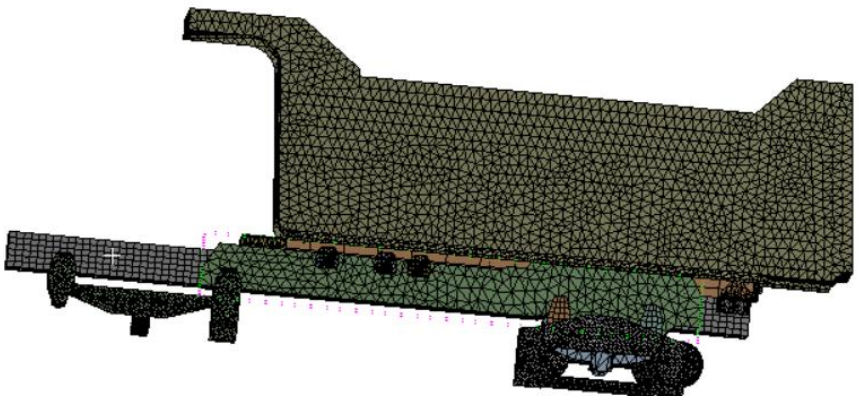

Fig. 4. Meshing diagram

4.2 Finite Element Analysis under Static Conditions

When the car is at rest, it is subjected to its own gravity and the load imposed by the heavy objects in the cargo carriage, according to the load calculation of 70t, and the cab is added to the load of 0.6t. The maximum deformation and the maximum internal stress under static conditions are calculated, and the results are shown in Fig. 5 and 6.

It can be seen from the figure that the maximum deformation is 1.13mm, the position is at the front of the carriage, the shape variable is obvious, the maximum concentrated stress is 80.3MPa, and the position is at the connecting plate between the bottom frame and the rear axle. The result of this analysis is 80.3MPa > 78.33MPa, and the frame is very unsafe at this time and needs to be optimized.

4.3 Finite Element Analysis under High-Speed Driving Conditions

According to the analysis in Chapter 3, under the condition of high-speed driving, the impact load on the bottom of the car is 105t, the impact load on the longitudinal beam of the lower frame increases to 0.9t, and the uniform load on all parts of the frame also increases to 1.05×10^6N, 9000N. The maximum deformation and maximum internal stress under high-speed driving conditions are calculated, and the results are shown in Figs. 7 and 8.

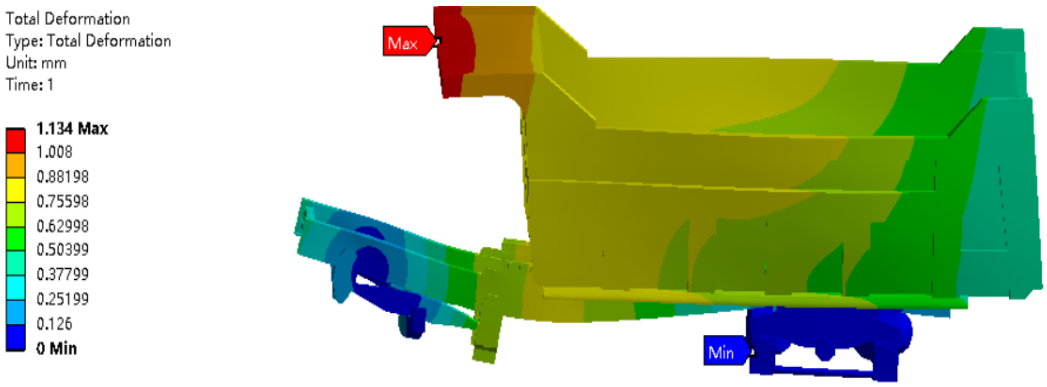

Fig. 5. Total deformation cloud image

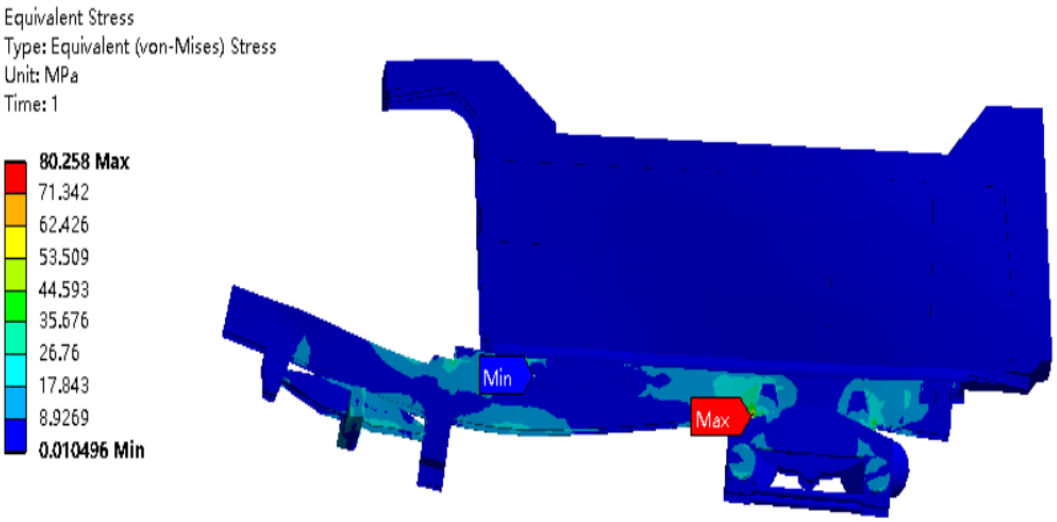

Fig. 6. Stress nephogram

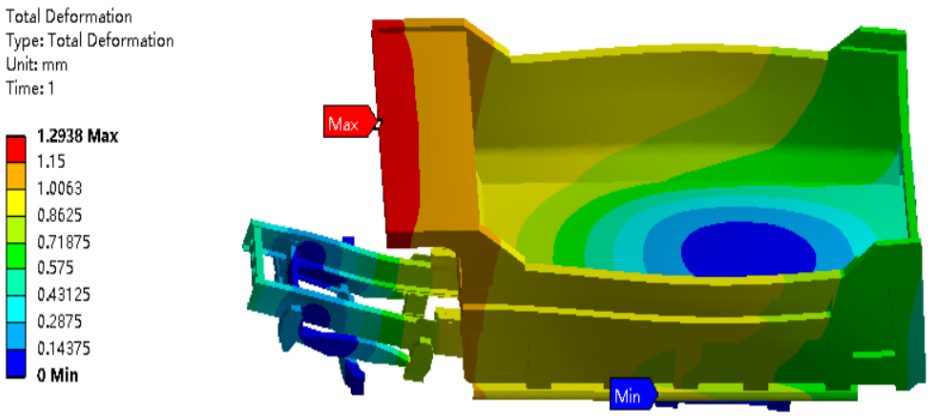

Fig. 7. Total deformation cloud image

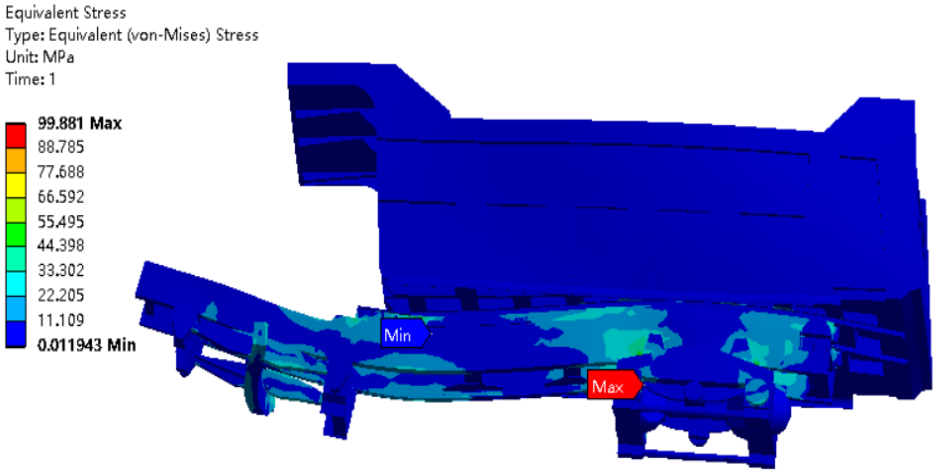

Fig. 8. Stress nephogram

It can be seen from the figure that the maximum deformation is 1.29mm, the position is at the front of the carriage, its shape variable is obvious, the maximum concentrated stress is 99.9MPa, and the position is at the connecting plate between the bottom frame and the rear axle. The result of this analysis is 99.9MPa > 78.33MPa, and the frame is very unsafe at this time, and needs to be optimized.

4.4 Finite Element Analysis under Turning Conditions

According to the analysis in Chapter 2, under the condition of high-speed driving, the impact load on the bottom of the car is 105t, the impact load on the longitudinal beam of the lower frame increases to 0.9t, and the uniform load on all parts of the frame correspondingly increases to 1.05×10^6N, 9000N, and the acceleration orientation to the left is 2m/s^2. The force on the bottom of the carriage is 1.05×10^6N longitudinally, the side force is 210000N, the force on the cab of the lower frame is 9000N longitudinally, and the side force is 1800N. The maximum deformation and maximum internal stress under turning conditions were calculated, and the results were shown in Figs. 9 and 10.

As can be seen from the figure, the maximum deformation is 1.48mm, the position is at the front of the carriage, its shape variable is obvious, the maximum concentrated stress is 107.8MPa, and the position is at the connecting plate between the underframe and the rear axle. Because the safety factor is 3, the result of this analysis is 107.8MPa > 78.33MPa, and the frame is unsafe and needs to be optimized.

5. OPTIMAL DESIGN OF FRAME BODY STRUCTURE

In the process of local optimization of the model, different methods were adopted, such as thickening, changing the shape, adding plates to increase the contact area, etc. Finally, it was concluded that the optimal solution to eliminate stress concentration was when the two sides of the rectangular shape of the connecting plate were widened into trapezoidal shape. The same method is also adopted for the position where the shape variable of the front end of the carriage is large, and the optimal scheme obtained is thickening the support plate.

In the end, the total weight of the scheme is increased by 90.35kg, and when the increased weight accounts for 0.9% of the total weight, the stress at the stress concentration location is reduced to 60.2MPa, 75.8MPa and 65.5MPa respectively under three different working conditions, which meet the safety standards and have sufficient margin, thus saving the use of raw materials [10]. At the same time, the overall structure of the frame is not changed, and the optimized rear compartment model is shown in Fig. 11.

After optimization, the total deformation cloud image under the three working conditions is shown in Fig. 12.

5.1 Conditions

After optimization, the local stress nephogram at the stress concentration under the three working conditions is shown in Fig. 13.

After optimization, the requirements are met under the three working conditions, and the total deformation and stress changes under the three working conditions are shown in Table 1.

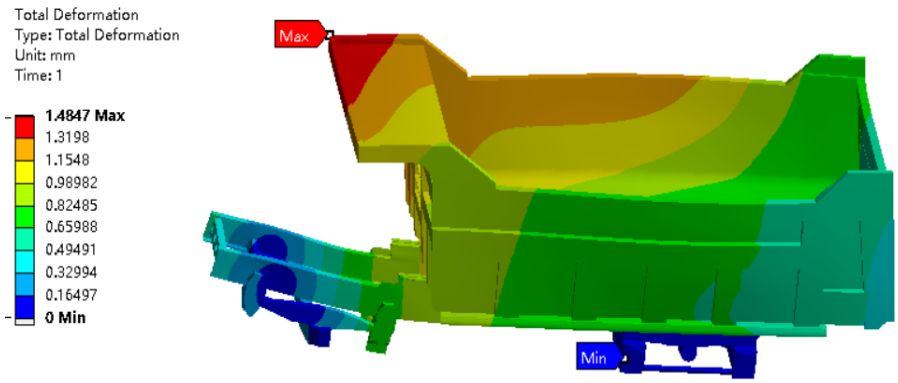

Fig. 9. Total deformation cloud image

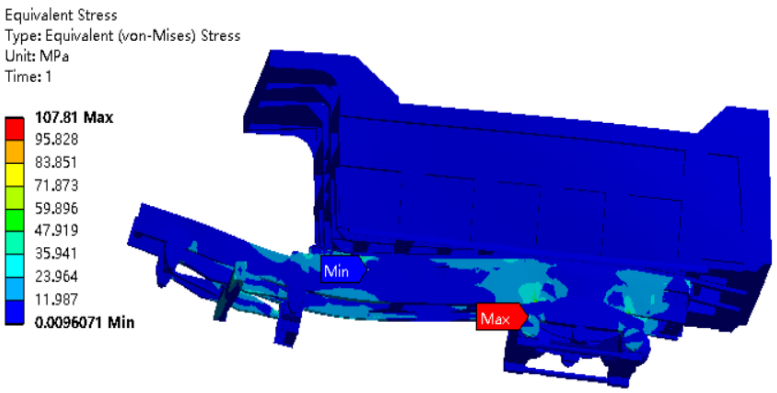

Fig. 10. Stress nephogram

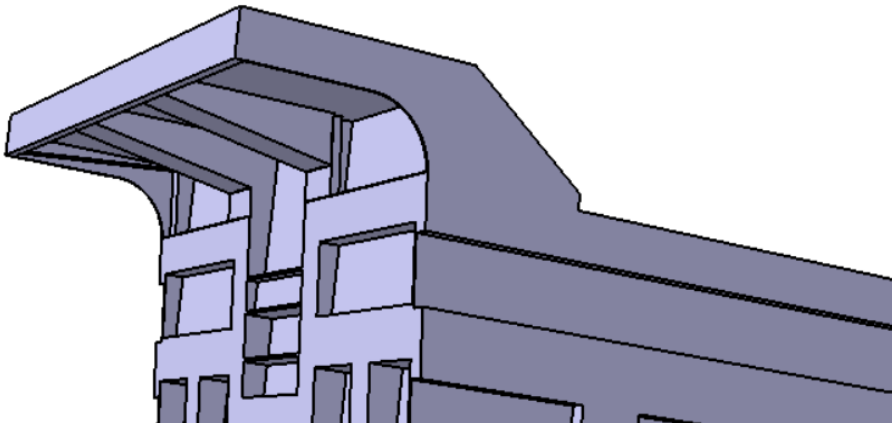

Fig. 11. Car Optimization model diagram

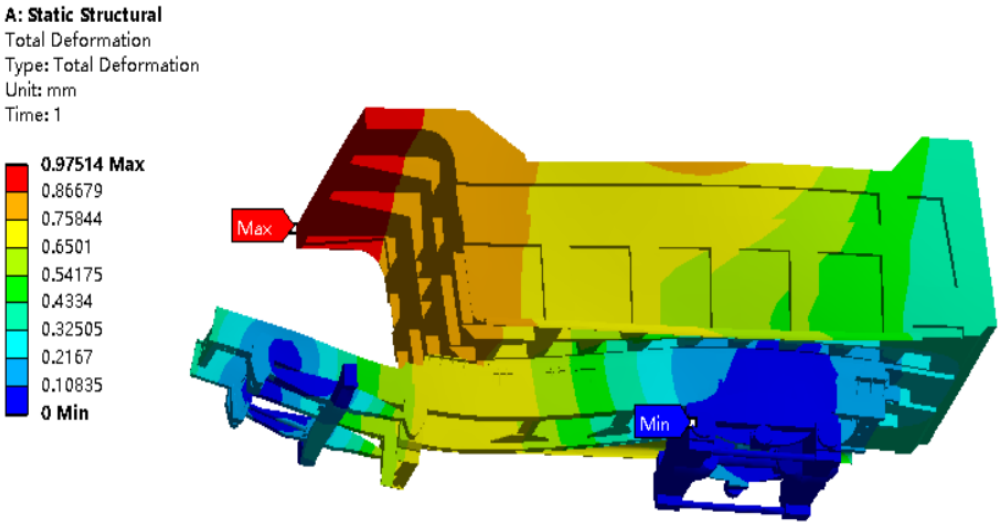

(a) Total deformation cloud image at rest

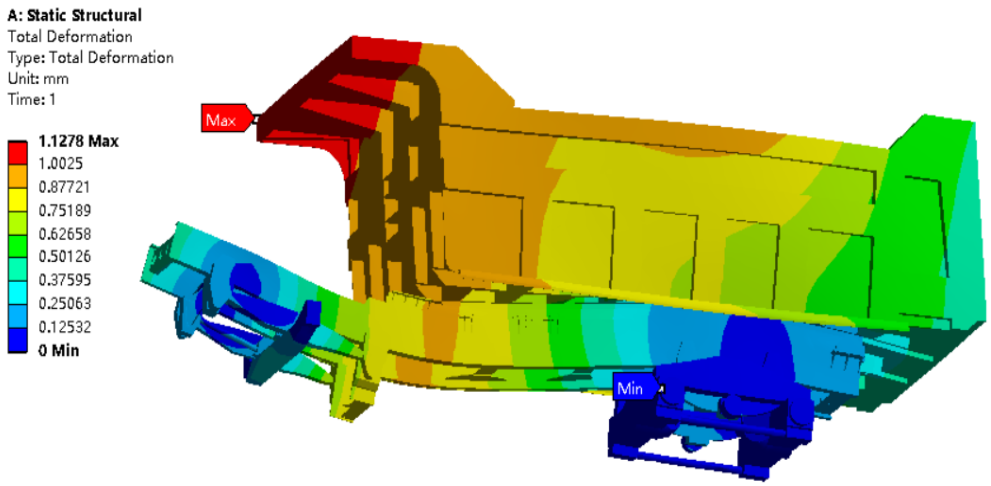

(b) Total deformation cloud image at high speed

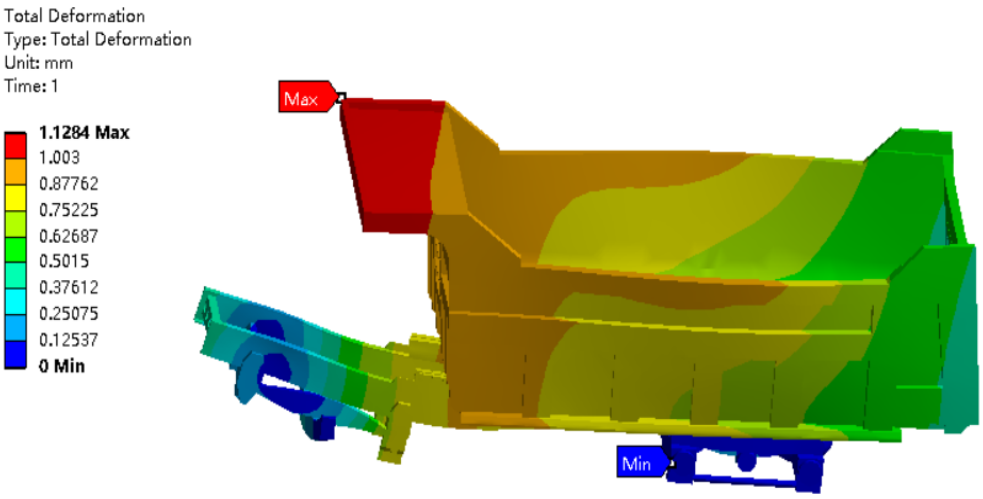

(c) Total deformation cloud image under turning condition

Fig. 12. Total deformation cloud image under different working

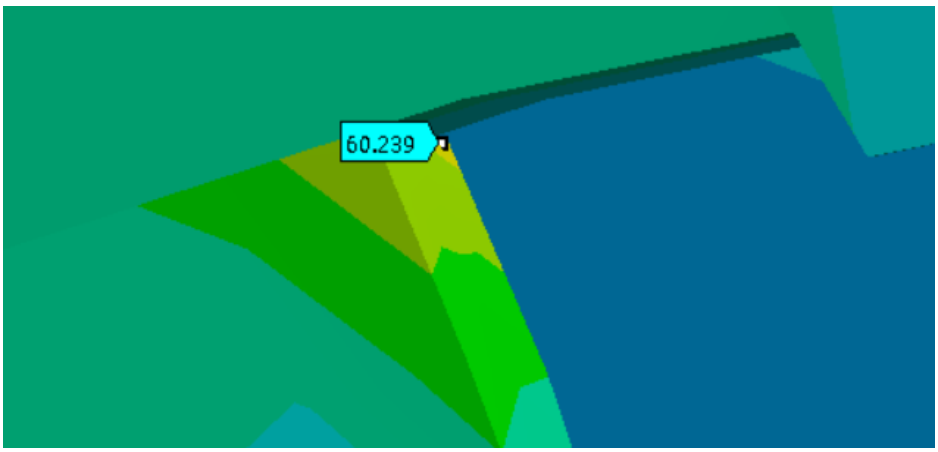

(a) Local stress nephogram under static conditions

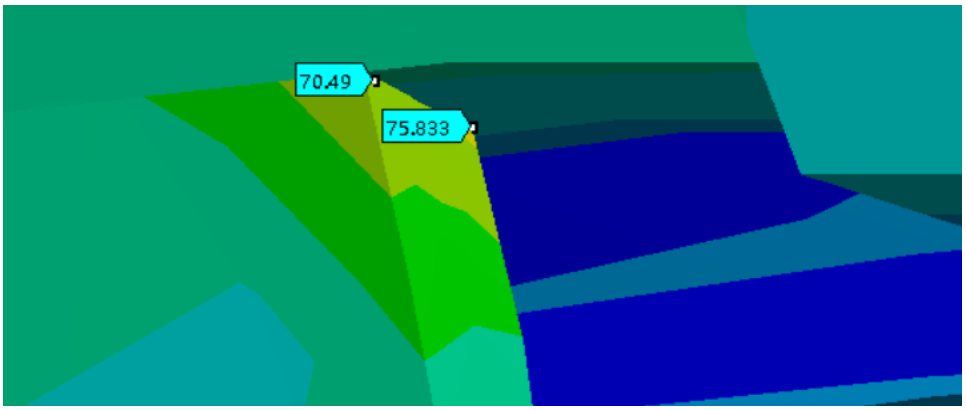

(b) Local stress nephogram under high speed driving conditions

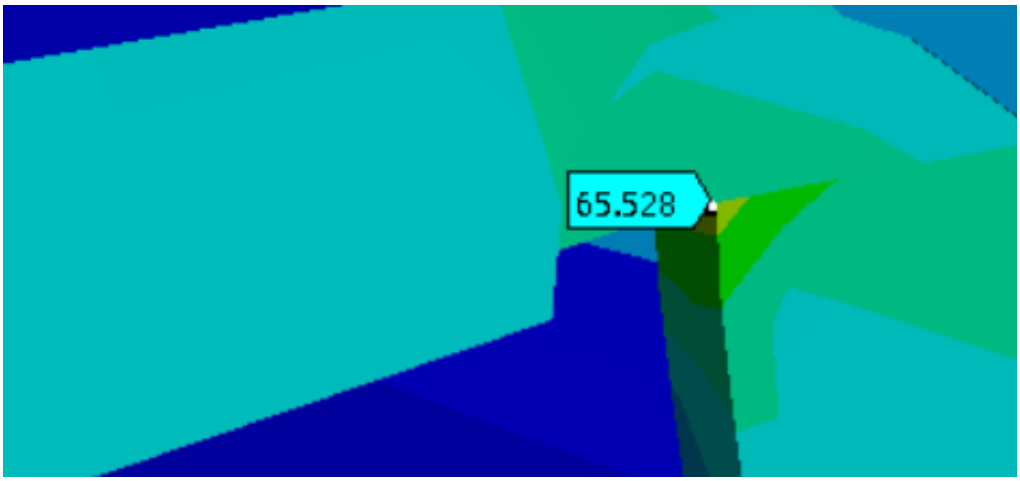

(c) Local stress nephogram under turning condition

Fig. 13. Stress cloud map at stress concentration

Table 1 Changes under three working conditions

Variable quantity operating condition	Stationary condition	High speed driving condition	Turning condition
Shape variable (mm)	-0.15	-0.16	-0.35
Stress（M Pa）	-20.1	-24.1	-42.3

6. CONCLUSION

This design takes the 60T electric mine vehicle frame and carriage as the research object, completes the model establishment, the simulation analysis under different working conditions, the design optimization and the check analysis after optimization.

The improvement method for the front end of the carriage with large deformation is to thicken the support plate at the lower part, and the support plate is thickened from 100mm to 300mm; The width of the connecting plate between the rear axle and the lower frame where the stress is concentrated is widened from a rectangular shape to a trapezoid. Specifically, the width of each side is widened to 30mm, and the total weight is increased by 90.35kg, accounting for 0.9% of the total weight. After optimization, the stress of the three working conditions is reduced by 25%, 24.1% and 39.2% respectively, and the frame and body meet the safety standards and the safety margin is sufficient.The simulation and optimization results can provide reference for the design of 60T pure electric mine vehicle frame and improve its safety and economy.

COMPETING INTERESTS

Author has declared that no competing interests exist.

REFERENCES

1. Yuan Min. Cao Fenghong. Zheng Caiguo et al. Topology optimization of pure electric mining truck frame [J]. Coal Mine Machinery. 2017;38(9):75-77.
2. Shi Xuanyu. Niu Zhigang. Zhu Xiaopeng. Modeling and Energy Consumption Analysis of electric rubber wheel Vehicle for Mining Based on Simulink [J]. Coal Engineering. 2015;53(1):166-171.
3. Czerwinski F. Current trends in automotive lightweighting strategies and materials. Materials. 2021;14(21):6631.
4. Zhang Wei. Yang Jue. Zhang Wenming et al. Research on compound energy system of pure electric mine car [J]. Automotive Engineering. 2019;41(6):641-653.
5. WANG Zhuozhou, Yao Xibin, Fu Ze, et al. Electric mine card based on the actual condition of energy efficiency analysis [J]. Chinese Mining Engineering. 2023,52(4): 81-86.

6. Han Nedan. Zhao Yang. Dong Xianchun et al. Lightweight and finite element simulation of mining dump truck [J]. Mechanical Engineering and Automation, 2018;6:208:78-83.
7. Han Zhilong. Feng Qiqing. Liu Kun. Electric Mining Car [P]. State Intellectual Property Office of the Republic of China. CN 211731013 U; 2020.10.23.
8. Tian Yuanwu, Yang Zhiwen, Wang Jiguang, et al. Based on k-means clustering of tianjin sanitation vehicle driving cycle research [J]. Journal of Hebei University of Technology. 2023;52(6):90-96.
9. Li Zhenjiang. Frame Design of Light Electric Truck [J]. Beijing Automobile. 2017;6:20-26.
10. Yu Yuzhen, Li Zhibin, Dong Xiaolei et al. Optimization design and analysis of micro-electric vehicle frame structure [J]. Manufacturing Automation. 2015;01:37(1): 135-138.

Peer-review history:
The peer review history for this paper can be accessed here:
https://www.sdiarticle5.com/review-history/116068